Protist, Vol. 170, 125680, November 2019
http://www.elsevier.de/protis
Published online date 30 August 2019

Protist

ORIGINAL PAPER

Gertia stigmatica gen. et sp. nov. (Kareniaceae, Dinophyceae), a New Marine Unarmored Dinoflagellate Possessing the Peridinin-type Chloroplast with an Eyespot

Kazuya Takahashi[a], **Garry Benico**[b], **Wai Mun Lum**[b], and **Mitsunori Iwataki**[a,1]

[a]Asian Natural Environmental Science Center, University of Tokyo, 1-1-1 Yayoi, Bunkyo, Tokyo 113-8657, Japan
[b]Graduate School of Agricultural and Life Sciences, University of Tokyo, 1-1-1 Yayoi, Bunkyo, Tokyo 113-8657, Japan

Submitted April 19, 2019; Accepted August 27, 2019
Monitoring Editor: Chris Howe

Marine unarmored dinoflagellates in the family Kareniaceae are known to possess chloroplasts of haptophyte origin, which contain fucoxanthin and its derivatives as major carotenoids, and lack peridinin. In the present study, the first species with the peridinin-type chloroplast in this family, *Gertia stigmatica* gen. et sp. nov., is described on the basis of ultrastructure, photosynthetic pigment composition, and molecular phylogeny inferred from nucleus- and chloroplast-encoded genes. Cells of *G. stigmatica* were small and harboring a chloroplast with an eyespot and two pyrenoids. The apical structure complex was straight, similar to *Karenia* and *Karlodinium*. Under transmission electron microscopy, the chloroplast was surrounded by two membranes, and the eyespot was composed of a single layer of osmiophilic globules (eyespot type A); this was never previously reported from the Kareniaceae. High performance liquid chromatography demonstrated the chloroplast contains peridinin, and neither fucoxanthin nor 19′-acyloxyfucoxanthins was identified. A phylogeny based on nucleus-encoded rDNAs suggested a position of *G. stigmatica* in the Kareniaceae, but not clustered within the previously described genera, i.e., *Karenia*, *Karlodinium* and *Takayama*. A phylogeny of chloroplast-encoded *psbA*, *psbC* and *psbD* indicated the chloroplast is of peridinin-type typical of dinoflagellates, but the most related species remains unclear.

Key words: Chloroplast; endosymbiosis; eyespot; *Gertia stigmatica*; Kareniaceae; peridinin.

Introduction

The family Kareniaceae is mainly comprised of three unarmored dinoflagellate genera, *Karenia*, *Karlodinium* and *Takayama* (Bergholtz et al. 2005; Daugbjerg et al. 2000; de Salas et al. 2008). One

[1]Corresponding author;
e-mail iwataki@anesc.u-tokyo.ac.jp (M. Iwataki).

https://doi.org/10.1016/j.protis.2019.125680

of characteristic features of this family is the shape of the furrow-like apical structure complex (ASC, = apical groove). Daugbjerg et al. (2000) described two genera with the straight ASC, *Karenia* and *Karlodinium*, the latter having a ventral pore and plug-like structure. De Salas et al. (2003) subsequently established the genus *Takayama* with a sigmoid ASC, showing a close relationship to *Karlodinium*. Recently, the affinity of *Asterodinium gracile* Sournia and *Brachidinium capitatum* F. J. R. Taylor to the Kareniaceae was demonstrated by molecular phylogeny, justifying the previous morphological observation of these species having a straight ASC (Benico et al. 2019; Gómez et al. 2005; Gómez 2006; Henrichs et al. 2011). Gómez et al. (2016) provided SSU rDNA sequence of *Ptychodiscus noctiluca* Stein, which similarly possesses a straight ASC, but its phylogenetic relationship to the Kareniaceae was not fully resolved. Members of the Kareniaceae, especially the three major genera, are recognized as fish-killing dinoflagellates (e.g., Dai et al. 2014; Leong et al. 2015; Lim et al. 2014; Onoue et al. 1985; Takayama 1981, 1985; Takayama and Matsuoka 1991; Takayama et al. 1998; Yang et al. 2000), and more than 30 species have so far been described (e.g., Bergholtz et al. 2005; Daugbjerg et al. 2000; de Salas et al. 2003, 2004, 2005, 2008; Gu et al. 2013; Haywood et al. 2004; Luo et al. 2018; Nézan et al. 2014; Yang et al. 2000, 2001).

Another diagnostic feature of the Kareniaceae is the possession of chloroplasts (i.e., photosynthetic plastids) containing fucoxanthin and 19′-acyloxyfucoxanthins (i.e., 19′-hexanoyloxyfucoxanthin and 19′-butanoyloxyfucoxanthin; 19′-AF-type) and lacking peridinin (e.g., Bergholtz et al. 2005; Bjørnland and Tangen 1979; Chang and Gall 2013; de Salas et al. 2003, 2004, 2005; Hansen et al. 2000; Tangen and Bjørnland 1981), which is different from the peridinin-type chloroplast typical in dinoflagellates. Phylogeny of plastid-encoded DNAs showed the kareniacean chloroplast to be of haptophyte origin (e.g., Gabrielsen et al. 2011; Ishida and Green 2002; Takishita et al. 1999, 2000, 2004, 2005; Tengs et al. 2000; Waller and Koreny 2017).

A naked dinoflagellate recently reported from the Ross Sea, Antarctic Ocean, does not have the typical chloroplast, even though it is closely related to the Kareniaceae in molecular analysis (Gast et al. 2006). According to Gast et al. (2007), this dinoflagellate possesses temporary chloroplasts (kleptochloroplasts) captured from the haptophyte *Phaeocystis* sp.; however, the phylogenetic position of this kleptochloroplast is not closely related to the permanent chloroplasts of *Karenia* and *Karlodinium* in the haptophyte clade. Similar isolates related to the Ross Sea dinoflagellate were also reported from the French coast (as Kareniaceae sp. in Nézan et al. 2014). These isolates are referred to as 'kleptoplastic sp.' in this article.

An interesting novel kareniacean species was isolated from the Japanese coast. This small marine dinoflagellate has the straight ASC of the Kareniaceae, but differs in having the peridinin-type chloroplast with an eyespot. In the present study, *Gertia stigmatica* gen. et sp. nov. is proposed for this isolate, with the description of its ultrastructure and pigment composition, and discussion of the evolutionary status on the basis of molecular phylogeny inferred from nucleus- and chloroplast-encoded DNAs.

Results

Family Kareniaceae Bergholtz, Daugbjerg, Moestrup et Fernández-Tejedor 2005

Gertia K. Takahashi et Iwataki gen. nov.

Unarmored dinoflagellates with chloroplast containing peridinin as a major pigment. Straight furrowed apical structure complex present.

Type species: *Gertia stigmatica* (described below).

Etymology: Named after Dr. Gert Hansen who proposed the genus *Karenia* Hansen et Moestrup ex Daugbjerg et al. (2000).

Gertia stigmatica K. Takahashi et Iwataki sp. nov.

Marine unarmored dinoflagellate. Cells ellipsoid, 5.9–9.5 μm long and 4.9–7.8 μm wide, with the epicone smaller than the hypocone. Cingulum anterior, displaced about one and a half cingulum width. Sulcus shallow. Nucleus situated in the hypocone. Chloroplast, brown in color, usually single and located mostly in the hypocone, with two stalked pyrenoids located left and right side in the hypocone, surrounded by a starch sheath. An eyespot composed of a single-layered osmiophilic globules (type A), located in sulcal region, present. Ventral pore absent.

Holotype: A preserved and dried specimen prepared from strain mdd472-kt on an SEM stub deposited in the Department of Botany, National Museum of Nature and Science, Tsukuba, as number TNS-AL-66002st.

Type Locality: Sagami Bay, Japan (35°09′N, 139°10′E).

Etymology: Named after the presence of an eyespot (= *stigma* in Greek).

Morphology and Ultrastructure

Cells of *Gertia stigmatica* were ellipsoid and measured 5.9–9.5 μm (mean 8.0 μm, n = 45) in length (Fig. 1A–H). The epicone was smaller than the hypocone, each measured 3.7−6.3 μm (mean 5.1 μm, n = 30) and 5.0−7.9 μm (mean 6.4 μm, n = 33) in width, respectively. The cingulum was situated slightly at the anterior, displaced ca. one and a half cingulum width (Fig. 1A, B). The sulcus was inconspicuous; the left side of the hypocone was slightly extended toward ventral, and the region around ventral ridge, which is usually found in the sulcus, formed a fine furrow structure (Fig. 1B). A straight furrowed apical structure complex (ASC) was observed in apico-ventral and apico-dorsal view (Fig. 1A, G). The right part of the epicone ventrally protruded in the lateral view (Fig. 1H). A brownish chloroplast was located mostly in the hypocone (Fig. 1C–F, H). The chloroplast was usually single, and sometimes split into several fragments (Fig. 1C–F, H, I). Autofluorescence of the chloroplast showed a lobed and roughly reticulated arrangement, at the periphery of the hypocone (Fig. 1J–L). Two stalked pyrenoids surrounded by a starch sheath, were observed at the left and right side in the hypocone (Fig. 1D, I). A reddish eyespot was situated in the sulcal region (Fig. 1C, H). An array of trichocysts running toward the antapex was observed in the hypocone (Fig. 1F). A dinokaryotic nucleus was spherical and located in the hypocone (Fig. 1H, L).

SEM showed small amphiesmal vesicles typical in unarmored dinoflagellates (Fig. 2A–H). The latitudinal series of vesicles were approx. 13; five on the epicone, three on the cingulum, and five on the hypocone (Fig. 2A–D, G). The anterior ridge of the cingulum was clearly seen in the lowermost series of epicone, which did not coincide with sutures of vesicle (Fig. 2B, G). The distal part of this ridge at the ventral side gradually disappeared (Fig. 2G). The posterior cingular margin was not apparent due to the lack of a distinct ridge (Fig. 2A, B, G). The ventral ridge was observed between the longitudinal and transverse flagellar insertions (Fig. 2A, E). A peduncle-like protrusion was found at the upper part of the ventral ridge (Fig. 2A, E). A copulation globe-like structure was observed on the ventral ridge, below the transverse flagellar insertion (Fig. 2E, F). The furrowed apical structure complex (ASC), 2.6 μm in mean length (n = 5), consisted of two straight ridges and a furrow between them (Fig. 2A–C, H). The left ridge of ASC was a row of seven knob vesicles, each containing usually two (sometimes three) globular knobs (Fig. 2A–C, H). The knob vesicles were surrounded by nine amphiesmal vesicles (Fig. 2H). The right ridge of the ASC, without knobs, was prominent (Fig. 2A–C, H).

Schematic illustrations of *G. stigmatica* are provided in Figure 3 based on morphological features under LM (Fig. 3A–C) and SEM (Fig. 3D–F).

Ultrastructure of *G. stigmatica* in TEM is shown in Figures 4 and 5. Longitudinal profile from the ventral side showed the relative position of chloroplast in the hypocone, two pyrenoids, a dinokaryotic nucleus and trichocysts mainly in the hypocone (Fig. 4A). Vacuoles similar in size were present at the periphery of the epicone and also at the antapical part of the hypocone (Fig. 4A). The chloroplast usually contained three-stacked thylakoids (Fig. 4B–F). The chloroplast envelope membranes, which are usually three in the peridinin-type chloroplast, were commonly two in number, under observation of both chloroplast and pyrenoid (Fig. 4B–D, F). No possible trace of the vestigial 19′-AF-type plastid was found. A stalked pyrenoid was surrounded by a starch sheath (Fig. 4A, E). An eyespot type A sensu Moestrup and Daugbjerg (2007), a single layer composed of four to eight osmiophilic globules in a section, was present in the chloroplast (Fig. 4G, H). A longitudinal microtubular strand (lmr, root 1) containing 11–13 microtubules, was identified between the eyespot and sulcus (Fig. 4G, H). The crystalline core of trichocysts was observed at the dorsal side of the eyespot (Fig. 4G). The plug-like structure, which was reported from *Karlodinium* (Bergholtz et al. 2005), was not observed around the amphiesmal vesicles (Fig. 4I).

In the ASC, one of the ridges with knob vesicles was supported by five microtubules and an electron opaque plate (op) (Fig. 5A), while the other ridge was supported by only an op (Fig. 5A). Several sheets underlying the furrow of ASC were observed (Fig. 5A).

The flagellar apparatus of *G. stigmatica* showed structures common in dinoflagellates; transverse and longitudinal basal bodies (tb and lb, respectively), lmr, transverse striated root (tsr, root 4), tsr microtubule (tsrm), striated root connective (src), and transverse and longitudinal striated collars (tsc and lsc, respectively) were identified (Fig. 5B–H). Two basal bodies were connected by two connectives (basal body connective 1 and 2; bbc_1 and

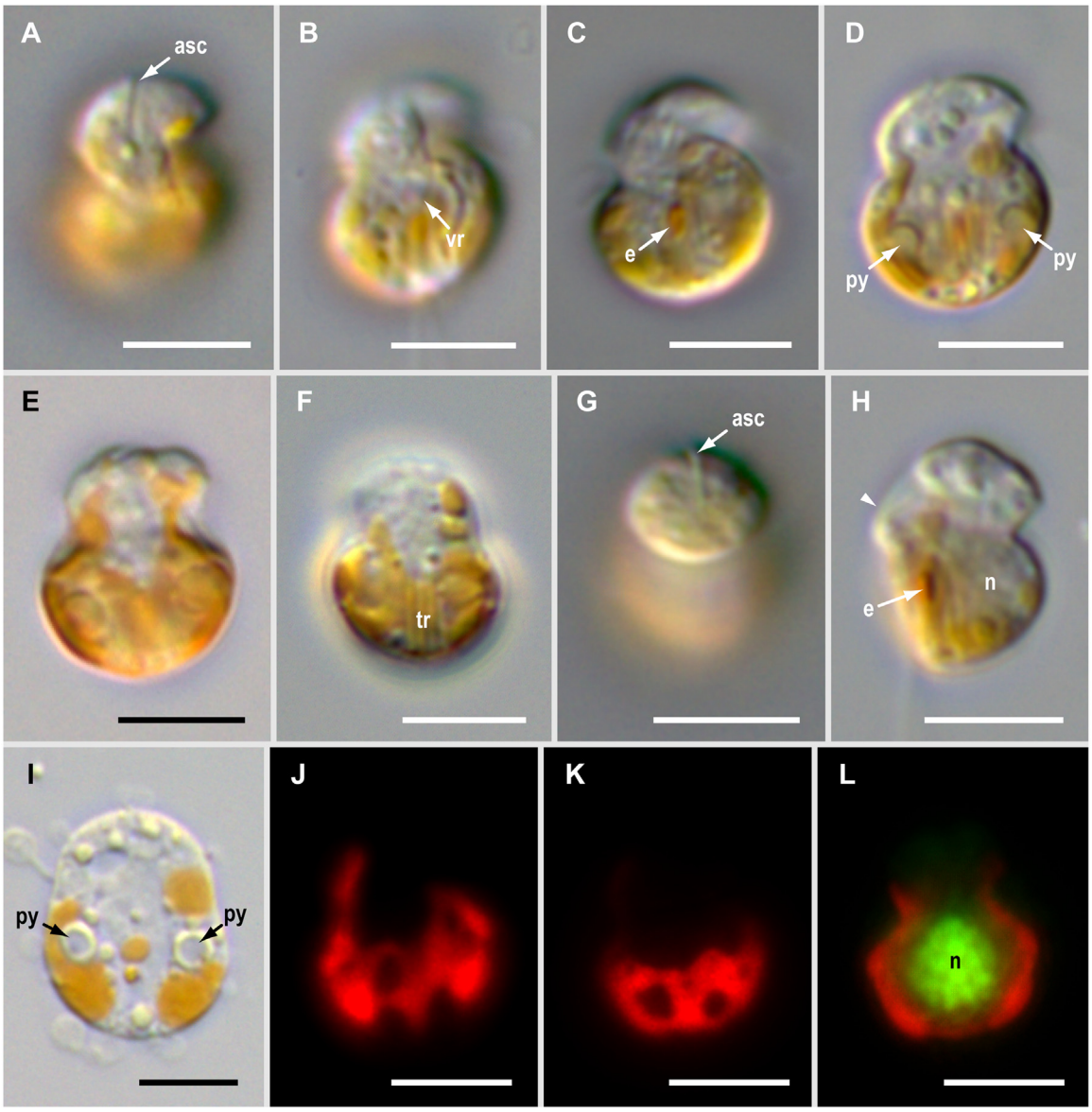

Figure 1. Light (**A–I**) and fluorescence (**J–L**) microscopy of *Gertia stigmatica* gen. et sp. nov. Scale bars = 5 μm. **A.** Ventral surface view showing straight apical structure complex (asc). **B.** Slightly deeper focus showing shallow sulcus and ventral ridge (vr). **C.** Deeper focus from ventral showing an eyespot (e) in the sulcal region. **D.** Deeper focus showing two pyrenoids (py). **E.** Chloroplast color similar to that of typical photosynthetic dinoflagellates. **F.** Deeper focus from dorsal showing trichocysts (tr) at antapex. **G.** Apico-dorsal surface showing straight apical structure complex (asc). **H.** Deeper focus in lateral view showing an eyespot (e) near the longitudinal flagellum, and a nucleus (n) in the hypocone. Arrowhead indicates protrusion of the epicone towards ventral. **I.** Compressed cell showing split chloroplast fragments different in sizes, and a starch sheath around the two pyrenoids. **J–L.** Autofluorescence of a chloroplast in different foci, from ventral surface (**J**), dorsal surface (**K**) and deep focus with a nucleus (n) (**L**).

bbc_2, respectively, Fig. 5B, E). A transverse microtubular root (tmr, root 3) was not shown, but a tmr extension (tmre)-like trace was observed at the upper part of the tb (Fig. 5C). Two pusules, comprising a round collecting chamber surrounded by several pusule vesicles, were observed at the upper and lower sides of flagellar apparatus (Fig. 5B). Two characteristic features, probably due to the small size of this species, were observed in the flagellar apparatus; first, the tsr was significantly thin, and

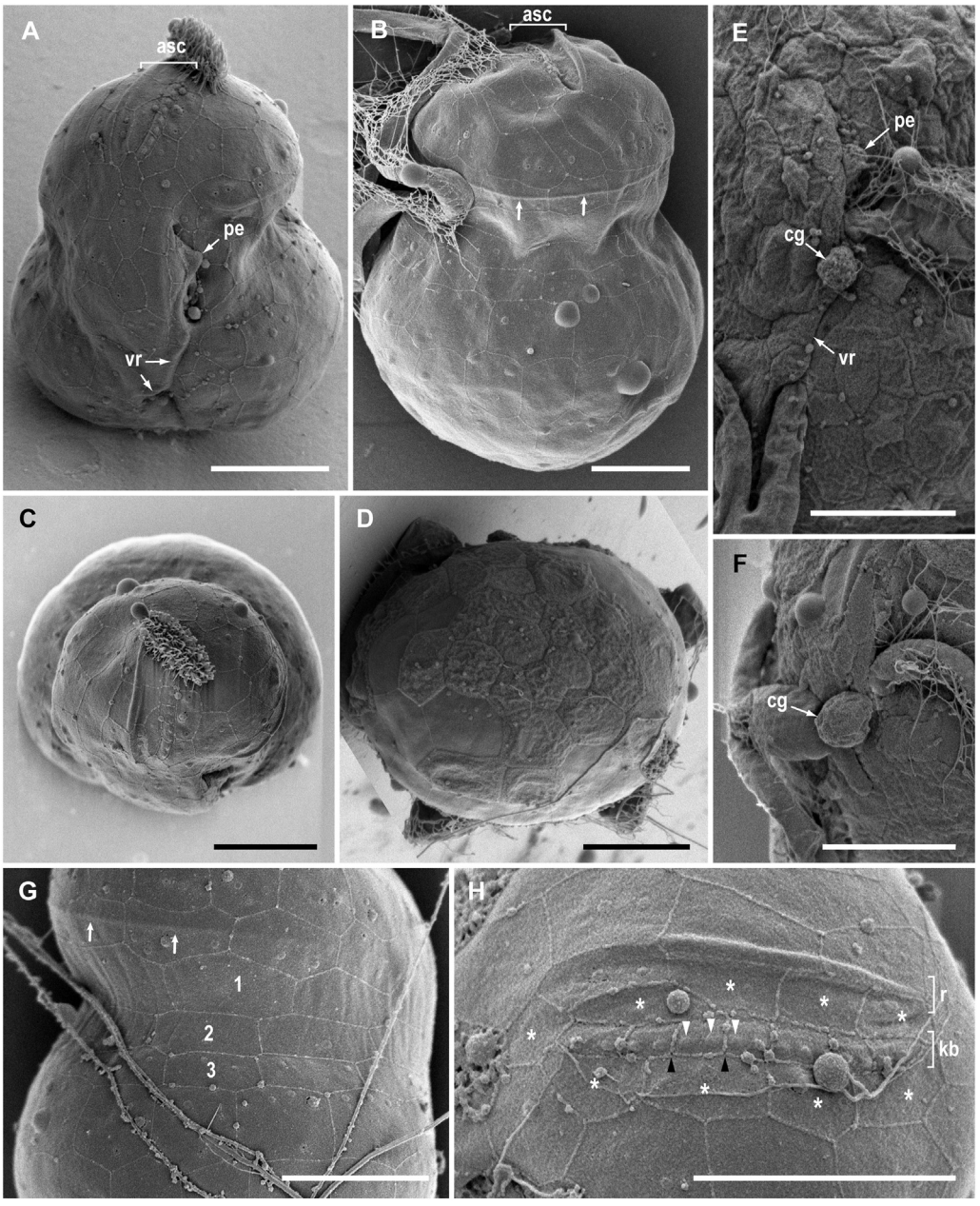

Figure 2. Scanning electron microscopy of *Gertia stigmatica* gen. et sp. nov. Scale bars = 2 μm. **A.** Apico-ventral view showing apical structure complex (asc), peduncle-like protrusion (pe) and ventral ridge (vr). Hairy structure on the asc is presumably a contaminated bacterium. **B.** Dorsal view showing anterior ridge of the cingulum (arrows). **C.** Apical view of the same cell in (A). **D.** Antapical view. **E.** Copulation globe-like structure (cg) at middle of vr path, different position from pe. **F.** Larger cg than that of (E). **G.** Right lateral view of the cingulum containing three rows of amphiesmal vesicles (1–3). Anterior ridge of the cingulum (arrows) disappearing toward the ventral. **H.** Amphiesmal vesicle arrangement around apical structure containing ridge (r) and knob vesicles (kb). Knob vesicles contain globular knobs (white arrowheads) and sutures (black arrowheads) and are surrounded by nine vesicles (asterisks).

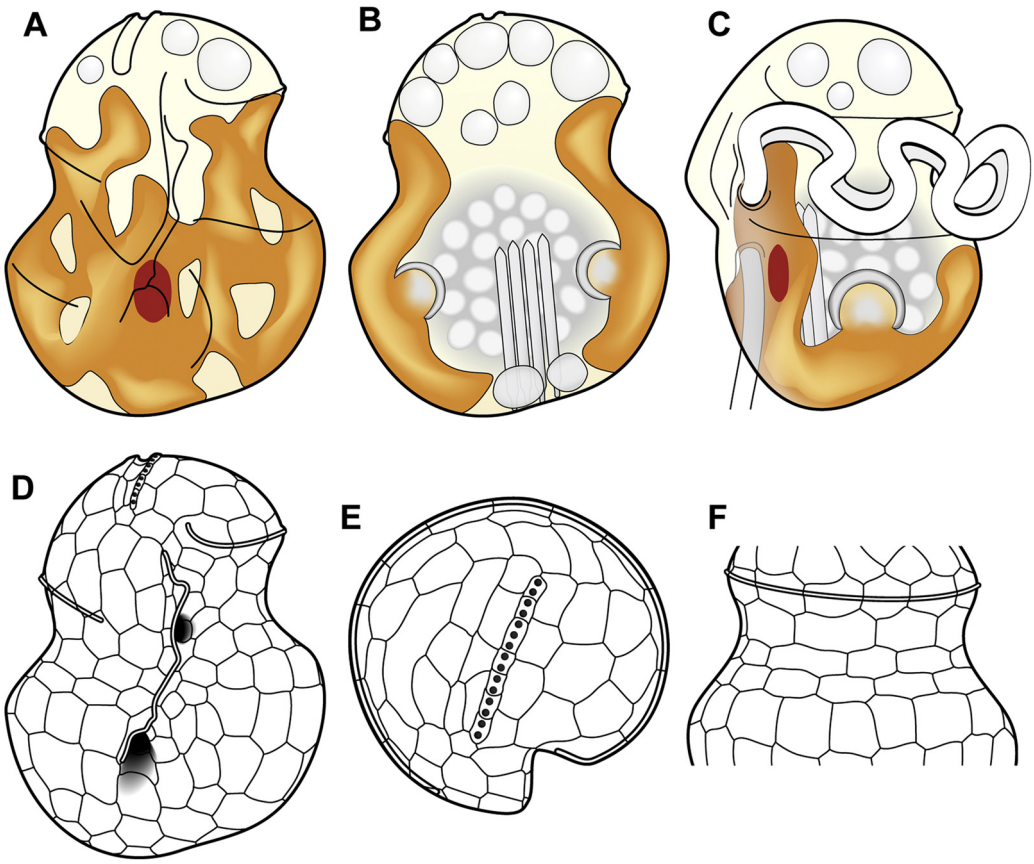

Figure 3. Schematic illustrations of *Gertia stigmatica* gen. et sp. nov. **A–C.** Cell contents including chloroplast, eyespot, nucleus and trichocysts. **A.** Ventral surface. **B.** Deeper profile from ventral. **C.** View from cell's left. **D–F.** Amphiesmal vesicle arrangements. **D.** Ventral view. **E.** Apical view. **F.** Cingulum from dorsal view.

its proximal part was measured approx. 35–40 nm in thickness (Fig. 5B). Second, the lmr was running in the lsc matrix, rather than its dorsal side, in the longitudinal section of the lateral view (Fig. 5F).

For other cytoskeleton structures, three to four microtubules, which correspond to the location of the ventral ridge seen in SEM (Fig. 2A, E), were observed at the cell's right side of the lmr (Fig. 4G, H). Around the level of two basal bodies, a fibrous component of ventral ridge (fvr) was also observed (Fig. 5D, F, H). Two microtubules, probably associated with the anterior ridge of the cingulum, were observed at the ventral side of the flagellar apparatus (Fig. 5G). The microtubular strand of peduncle (msp) was faint, around the projection of peduncle, at the upper part of the transverse flagellum (Fig. 5D).

Pigment Composition

Photosynthetic pigment compositions of *G. stigmatica*, *Heterocapsa circularisquama* Horiguchi (peridinin-type) and *Karenia mikimotoi* (Miyake et Kominami ex Oda) Gert Hansen et Moestrup (19′-AF-type) were compared in HPLC chromatograms (Fig. 6). Pigments commonly detected in the three dinoflagellates were chlorophyll c_2, chlorophyll *a*, chlorophyll *a* allomer and diadinoxanthin. In *G. stigmatica* and *H. circularisquama*, peridinin was detected as a major carotenoid. The three pigments, i.e., peridinin-like pigment, dinoxanthin and diadinochrome, were identified by absorption spectra (Roy et al. 2011) and relative retention times (Zapata et al. 2012), since there were no available standards. In the two peridinin-type species, β-carotene was detected only from *G. stigmatica*, and two unidentified pigments (pigments 7 and 9) were found only in *H. circularisquama*. Eight minor unidentified peaks (pigments 1, 2, 4–6, 14, 16, 17) were commonly observed in *G. stigmatica* and *H. circularisquama*, and were different from any peaks of *Karenia mikimotoi* (including unidentified pigments 3, 8, 10–13, 15, 18) in retention times and/or absorption spectra. Pigments of *Karenia mikimotoi*

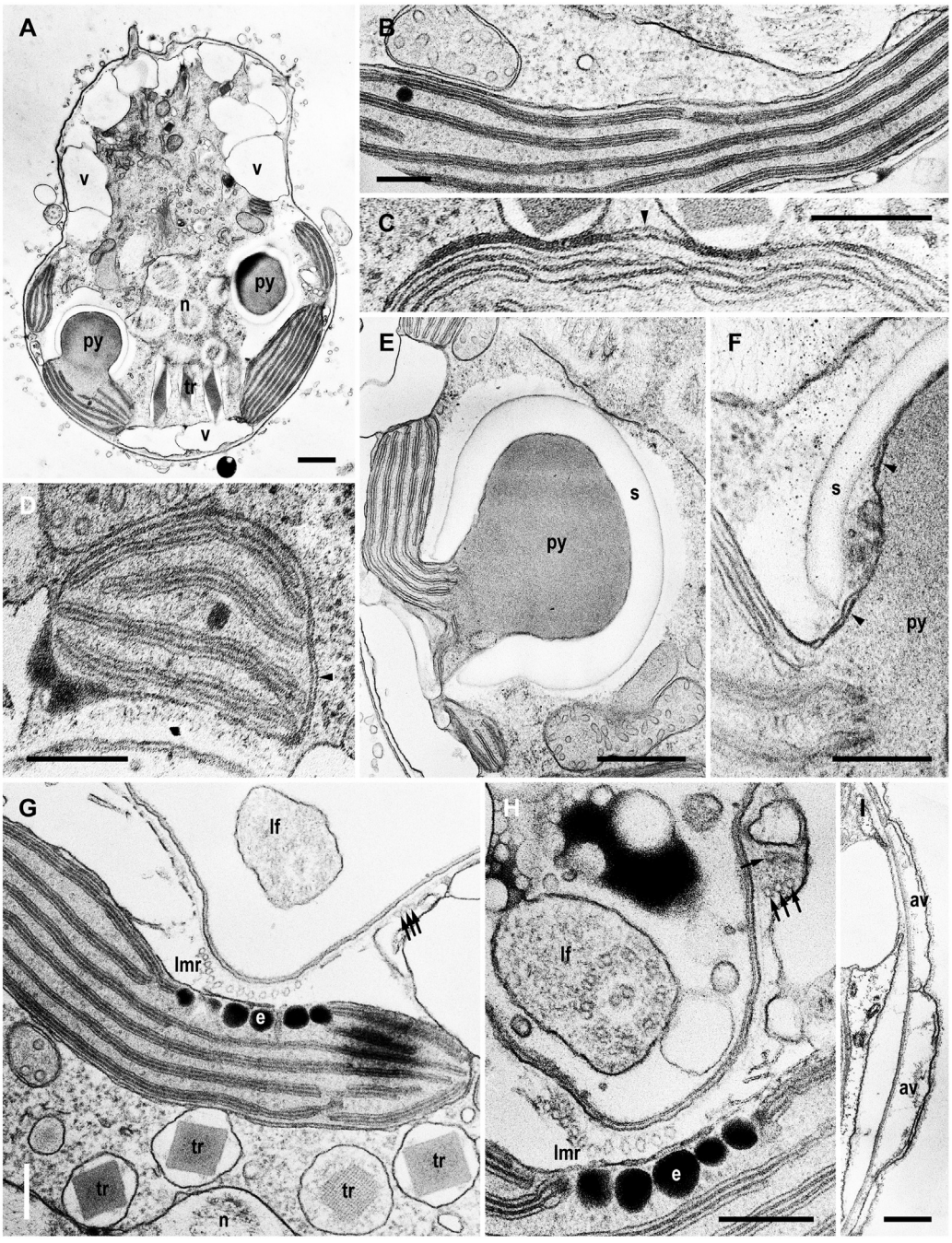

Figure 4. Transmission electron microscopy of *Gertia stigmatica* gen. et sp. nov. Scale bars =500 nm for A and E, 200 nm for B–D, and F–I. Schedule 1: A, C–F; schedule 2: B, G and H; schedule 3: I. **A.** Longitudinal section of ventral view showing pyrenoids (py) and vacuoles (v). **B–D.** Chloroplast bounded by double-membrane (arrowheads). **E.** A single starch sheath (s) surrounding a pyrenoid (py). **F.** Proximal region of pyrenoid with membranes (arrowheads) and a starch sheath (s). **G, H.** A single layer of eyespot (e) globules in chloroplast, facing longitudinal flagellum (lf) and longitudinal microtubular root (lmr). Trichocysts (tr) between chloroplast and nucleus (n), and microtubules (black arrows) probably supporting ventral ridge are also seen. **I.** Amphiesmal vesicles (av).

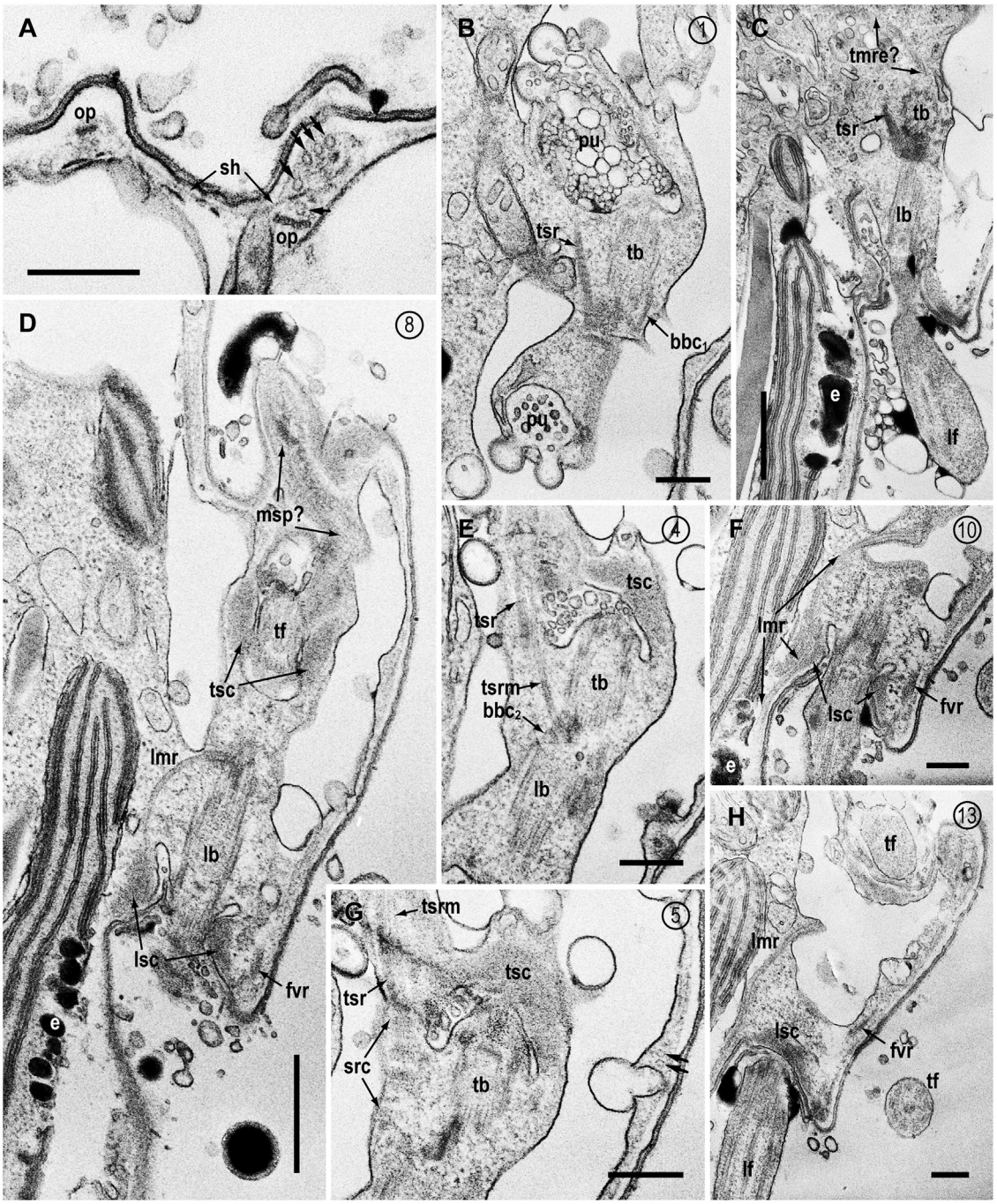

Figure 5. Transmission electron microscopy of *Gertia stigmatica* gen. et sp. nov. Scale bars =200 nm for A, B and E–H, 500 nm for C and D. Schedule 1: A and C; schedule 2: B and D–H. **A.** Section of apical structure complex showing five microtubules (arrows), sheet (sh) and two electron opaque plates (op). **B–H.** Lateral views of longitudinal section showing the flagellar apparatus. The encircled numbers are serial section number. **B.** Transverse basal body (tb), transverse striated root (tsr) and basal body connective 1 (bbc_1). Two pusules (pu) are also seen. **C.** Eyespot (e) globules positioned beside the longitudinal flagellum (lf) associated with longitudinal basal body (lb). Putative transverse microtubular root extension (tmre?) is seen above the tb. **D.** A structure resembling microtubular strand of peduncle (msp?) runs anterior, toward distal end of the peduncle. Transverse flagellum (tf), transverse striated collar (tsc), longitudinal striated collar (lsc), and fiber in ventral ridge (fvr) are seen. **E.** Transverse striated root microtubule (tsrm) associated with tsr runs from basal body connective 2 (bbc_2). **F.** The lmr runs through the lsc matrix. **G.** Striated root connective (src) associated with tsr. Two microtubules (arrows) are seen near the cell surface. **H.** The fvr runs toward anterior.

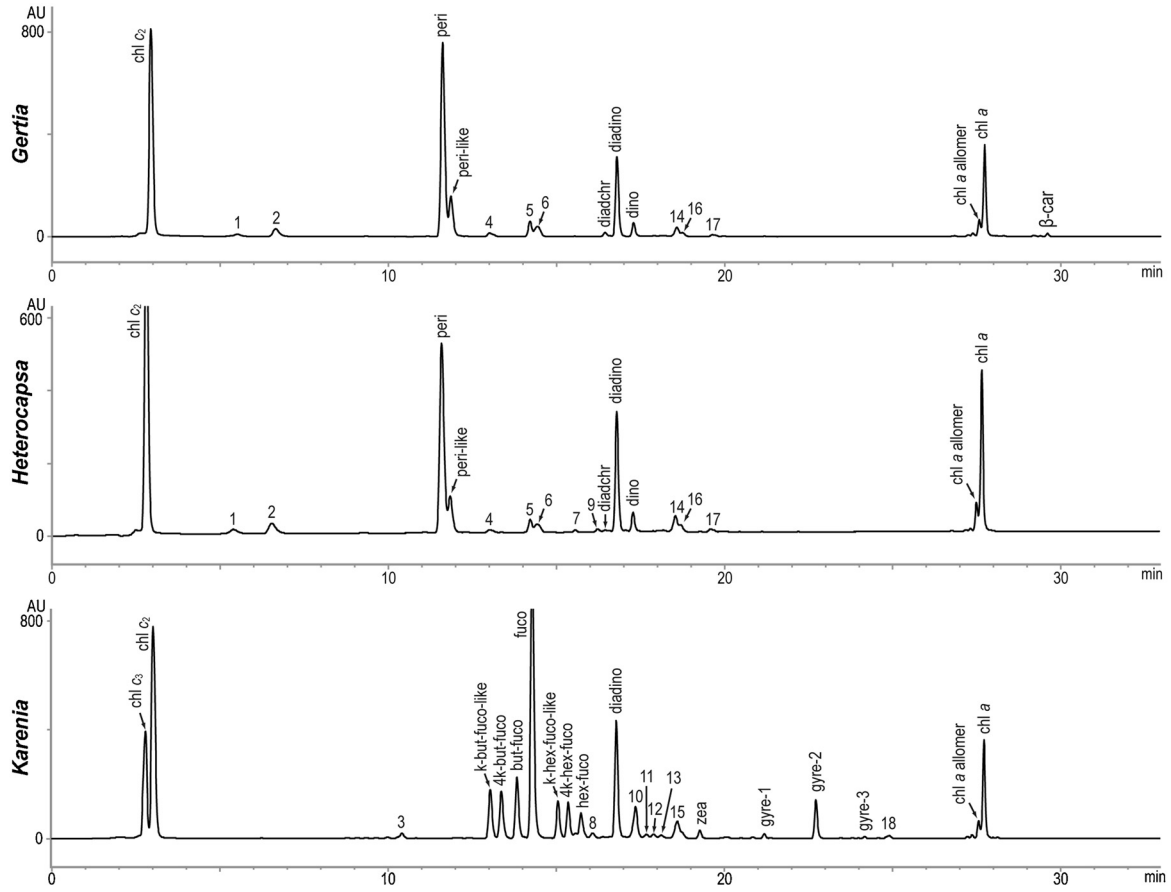

Figure 6. HPLC chromatograms of chloroplast pigments in *Gertia stigmatica* gen. et sp. nov., *Heterocapsa circularisquama* and *Karenia mikimotoi*. Absorption at wavelength 440 nm. Abbreviations: but-fuco, 19′-butanoyloxyfucoxanthin; chl *a*, chlorophyll *a*; chl c_2, chlorophyll c_2; chl c_3, chlorophyll c_3; diadchr, diadinochrome; diadino, diadinoxanthin; dino, dinoxanthin; fuco, fucoxanthin; gyre-1–3, gyroxanthin diester 1–3; hex-fuco, 19′-hexanoyloxyfucoxanthin; 4k-but-fuco, 4-keto-19′-butanoyloxyfucoxanthin; k-but-fuco-like, keto-19′-butanoyloxyfucoxanthin-like; 4k-hex-fuco, 4-keto-19′-hexanoyloxyfucoxanthin; k-hex-fuco-like, keto-19′-hexanoyloxyfucoxanthin-like; peri, peridinin; peri-like, peridinin-like; zea, zeaxanthin; β-car, β-carotene. Unidentified small peaks were labeled as pigments 1–18.

were identified according to Benico et al. (2019). This species contained chlorophyll c_3, fucoxanthin, two forms of 19′-acyloxyfucoxanthins, four forms of keto-acyloxyfucoxanthins, zeaxanthin and three gyroxanthin diesters. Pigments specific to the two kareniaceans, *G. stigmatica* and *Karenia mikimotoi*, were not identified.

Dinoflagellate Host and Chloroplast Phylogeny

To infer the phylogenetic position of the host dinoflagellate, nucleus-encoded SSU, ITS region and LSU rDNA sequences (4,925 bps) were determined from *G. stigmatica*, and compared with unarmored (e.g., *Amphidinium*, *Gymnodinium* and *Gyrodinium*), armored (e.g., Gonyaulacales, Dinophysiales, Peridiniales and Prorocentrales), and woloszynskioid (e.g., Suessiales) dinoflagellates. In rDNA trees, the general topology and position of *G. stigmatica* in Kareniaceae were not significantly different between maximum likelihood (ML) and Bayesian inference (BI), hence only BI trees are given. All kareniacean sequences including *G. stigmatica* formed a monophyletic group in the concatenated rDNA (posterior probability of BI/bootstrap support value of ML = 0.95/96%, Fig. 7A), SSU rDNA (<0.70/<50, Fig. 7B), ITS (1.00/99, Fig. 7C), and LSU rDNA (0.82/82, Fig. 7D). In the Kareniaceae clade, two robust sub-clades were recognized; one contained *Karenia* spp., *Brachidinium capitatum* and *Asterodinium gracile* (1.00/100 in concatenated, ITS and LSU,

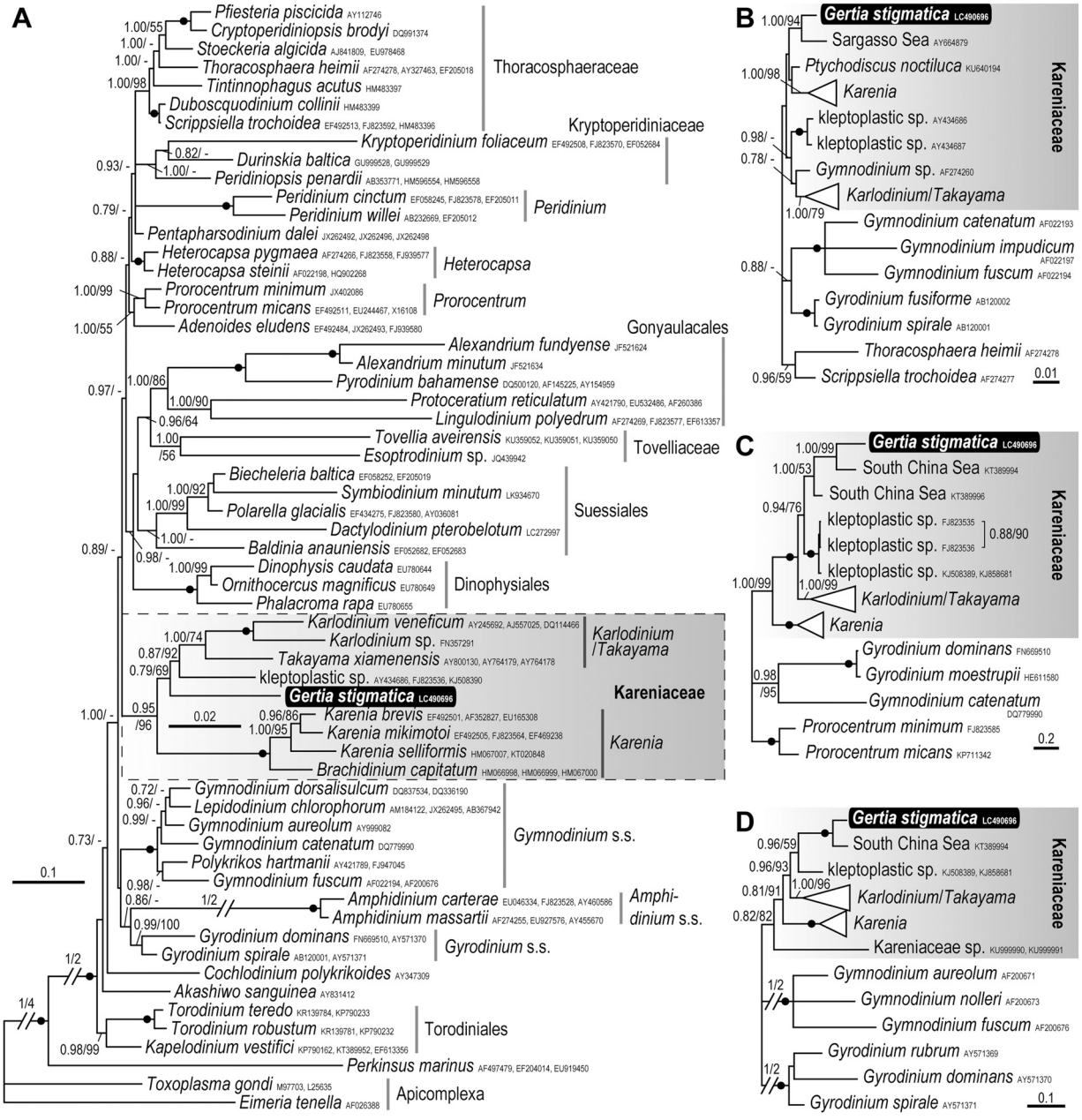

Figure 7. Bayesian inference (BI) phylogeny of *Gertia stigmatica* gen. et sp. nov. (highlighted in a black box) from nucleus-encoded SSU, ITS and partial LSU rDNA sequences. Posterior probability (PP $\geq$ 0.70) and bootstrap supports (BS) of maximum likelihood (ML) analysis ($\geq$50%) are shown in left and right, respectively. PP was based on 4,000,000 Markov Chain Monte Carlo (MCMC) generations for concatenated, 500,000 MCMC generations for SSU, ITS and LSU analyses, with sampling at every 500 generations for concatenated, 100 generations for SSU, ITS and LSU analyses. Black dot on the node indicates maximum supports (PP/BS = 1.00/100). Non-collapsed trees are available in Figure S1 (SSU), S2 (ITS) and S3 (LSU). **A.** Concatenated tree of SSU, 5.8S of ITS and LSU without partial D2 (3,441 characters of 60 sequences). Substitution model was GTR + G (= 0.4748) + I (= 0.2736). Note that scale bar in the Kareniaceae is different from that of other sequences (branches were five times longer, in a square with dashed line). **B.** SSU phylogeny (1,760 characters of 35 sequences). Substitution model was GTR + G (= 0.6623) + I (= 0.6722). **C.** ITS phylogeny (ITS1, 5.8S and ITS2, 751 characters of 58 sequences). Substitution model was GTR + G (= 1.2117) + I (= 0.2603). **D.** LSU phylogeny (including whole D2 region, 985 characters of 71 sequences). Substitution model was GTR + G (= 0.5134) + I (= 0.2786).

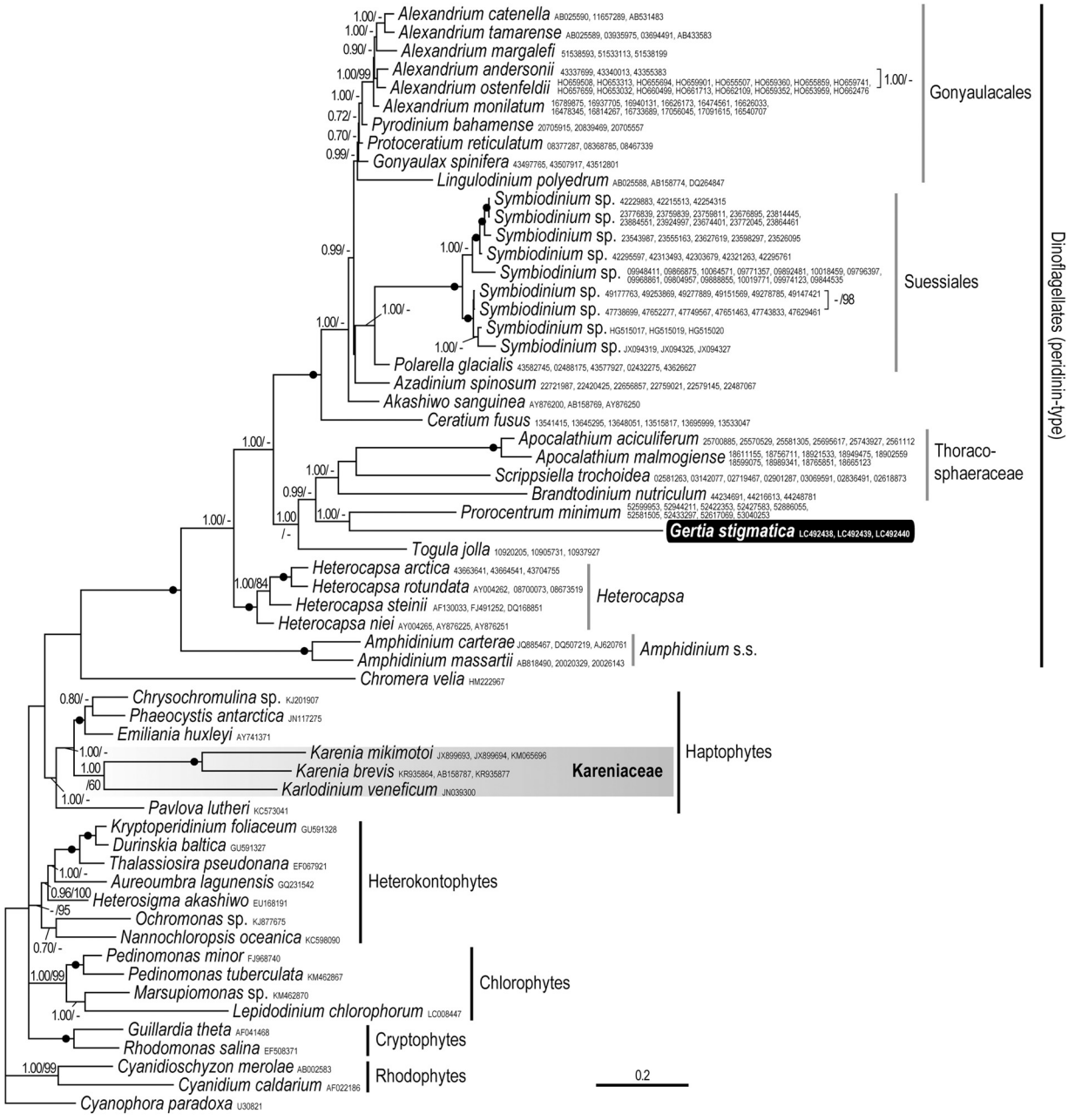

Figure 8. Bayesian inference (BI) phylogeny of *Gertia stigmatica* gen. et sp. nov. (highlighted in a black box) from concatenated chloroplast-gene sequences (*psbA-psbC-psbD*, 3,426 characters of 60 sequences). 8-digit numeral numbers indicate sequences sourced from iMicrobe (CAMNT 00), and 6–8-digit numbers starting with one or two alphabets are sequences obtained from GenBank. *Cyanophora paradoxa* (U30821) was defined as an outgroup. Substitution model was GTR + G (= 0.8746) + I (= 0.2665). Posterior probabilities (PP) were calculated by 10,000,000 MCMC generations with sampling trees of every 100 generations. PP (≥0.70) and bootstrap values of maximum likelihood analysis (≥50%) are shown in left and right, respectively. Black dot on the node indicates maximum supports (PP/BS = 1.00/100).

1.00/98 in SSU), and the other contained *Karlodinium* spp. and *Takayama* spp. (1.00/74 in concatenated, 1.00/79 in SSU, 1.00/99 in ITS, 1.00/96 in LSU) (Fig. 7A–D; Supplementary Material Figs S1–S3). *Gertia stigmatica* was included in neither of the two sub-clades, and relatively close to kleptoplastic sp. The position of *G. stigmatica* in relation to kleptoplastic sp. differed in the concatenated tree, SSU, ITS and LSU trees. In the concatenated tree, kleptoplastic sp. was a sister to *Karlodinium*/*Takayama* (0.87/92) and *G. stigmatica* branched at their basal position (0.79/69) (Fig. 7A). In the SSU tree, *G. stigmatica* was related to an environmental sequence from the Sargasso Sea (AY664879), and their relationships to *Karenia*, *Karlodinium*/*Takayama*, and kleptoplastic sp. were unclear (Fig. 7B). *Gertia stigmatica* was most closely related to the two environmental sequences from the South China Sea (KT389994, KT389996) both in ITS (1.00/53) and LSU (1.00/100). This clade was a sister to kleptoplastic sp. in ITS (0.94/76) and LSU (0.93/59), and they were consequently sister to *Karlodinium*/*Takayama* in ITS (1.00/100) and LSU (0.96/93) (Fig. 7C, D). The ambiguous position of *G. stigmatica* in SSU tree as compared to ITS and LSU trees was due to the smaller number of variable sites; parsimony-informative sites identified by MEGA were 76/1,760 sites in SSU, 357/766 sites in ITS and 225/990 sites in LSU, within the Kareniaceae. The sister relationship of *Karenia* and *Karlodinium*/*Takayama* was not shown in any nucleus-encoded datasets, and *G. stigmatica* always positioned between them (Fig. 7A–D).

To infer the phylogenetic position of the chloroplast, chloroplast-encoded *psbA* (786 bps), *psbC* (698 bps), and *psbD* (904 bps) were determined from *G. stigmatica*, and compared with the dinoflagellate chloroplast genes of peridinin-type, 19′-AF-type, fucoxanthin-type (Kryptoperidiniaceae) and chlorophyll *b*-type (*Lepidodinium chlorophorum* (Elbrächter et Schnepf) Hansen, Botes et de Salas), as well as those of haptophytes, heterokontophytes, cryptophytes and chlorophytes (Fig. 8; Supplementary Material Figs S4–S6). Since BI and ML showed no significant topological differences, only BI trees are shown in Figure 8 (concatenated tree), S4 (*psbA*), S5 (*psbC*) and S6 (*psbD*). Dinoflagellates with the peridinin-type chloroplast, including *G. stigmatica*, formed a well-supported clade (1.00/100 in concatenated, 1.00/96 in *psbA*, 1.00/99 in *psbC* and 1.00/91 in *psbD*). Dinoflagellates with the 19′-AF-type chloroplast, *Karenia mikimotoi*, *Karenia brevis* (C.C. Davis) Gert Hansen et Moestrup and *Karlodinium veneficum* (D. Ballantine) J. Larsen, formed a clade (1.00/60 in concatenated, 0.97/62 in *psbA*, 1.00/<50 in *psbC*, and 0.80/<50 in *psbD*) in haptophytes (1.00/<50 in concatenated and *psbA*, 0.73/<50 in *psbC*, and 0.77/<50 in *psbD*) (Figs 8, S4–S6). The definitive position of *G. stigmatica* chloroplast was not determined; the sister was *Prorocentrum minimum* (Pavillard) Schiller in the concatenated tree (1.00/<50, Fig. 8), *Nematodinium* sp. in the *psbA* tree (0.79/<50, Supplementary Material Fig. S4), *Pelagodinium bei* (Spero) Siano, Montresor, Probert et Vargas in the *psbC* tree (<0.70/<50, Supplementary Material Fig. S5), and *Togula jolla* Flø Jørgensen, Murray et Daugbjerg in the *psbD* tree (0.99/<50, Supplementary Material Fig. S6).

To examine the presence of 19′-AF-type chloroplast in *G. stigmatica*, amplifications of chloroplast-encoded 16S rDNA and *rbcL* gene (form I) were attempted, by using the primers sensitive to 16S rDNA of *A. gracile* (Benico et al. 2019) and to *rbcL* of *Karenia mikimotoi* (Al-Kandari et al. 2011), in addition to newly designed primers (Supplementary Material Table S1). No sign of 16S rDNA and *rbcL* amplification was detected from *G. stigmatica*.

Discussion

Taxonomy

Gertia stigmatica possesses the straight ASC, the character shared with *Karenia* and *Karlodinium*, and its position in the Kareniaceae was supported by nucleus-encoded rDNA phylogenies. On the other hand, the chloroplast found in *G. stigmatica* was of peridinin-type, which is distinct from 19′-AF-type reported in other kareniacean species (Benico et al. 2019; Daugbjerg et al. 2000; de Salas et al. 2003). This pigment composition does not correspond with the diagnosis of the family Kareniaceae defined by having acyloxyfucoxanthins and lacking peridinin (Bergholtz et al. 2005). A similar case was previously reported in an unarmored dinoflagellate *Lepidodinium* in the Gymnodiniaceae, which possesses the horseshoe-shaped ASC and phylogenetically related to *Gymnodinium* sensu stricto, but it has the unusual chloroplast of green algal origin (Elbrächter and Schnepf 1996; Hansen and Moestrup 2005; Hansen et al. 2007; Watanabe et al. 1987, 1990). We therefore provisionally assign the species *G. stigmatica* to the family Kareniaceae, as the first member possessing the peridinin-type chloroplast.

Gertia stigmatica is a small marine unarmored dinoflagellate with the large hypocone harboring

a nucleus, a brown chloroplast and an eyespot. Similar unarmored species are *Gymnodinium cinctum* Kofoid et Swezy, *Amphidinium lissae* Schiller and *Gymnodinium parvum* Larsen (Kofoid and Swezy 1921; Larsen 1994; Schiller 1933). *Gymnodinium cinctum* has chloroplasts, the ratio of cell length/width 1.18 (1.18–1.20 in *G. stigmatica*), and the cingulum displaces more than one of its own width (Kofoid and Swezy 1921); however, the species is large (25 μm) and lacks an eyespot. *Amphidinium lissae* has chloroplasts and an eyespot (Schiller 1933), but its cingulum has no displacement. Since the chloroplast was described to be green (Schiller 1933), *A. lissae* could be a member of the genus *Nusuttodinium*, which possesses blue-green kleptochloroplasts from cryptophytes, and sometimes an eyespot-like orange colored structure (Takano et al. 2014). The straight ASC and trichocyst-like rods in the hypocone were reported in *G. parvum*, but this is a heterotrophic and slightly large species (15 μm long) (Larsen 1994).

Chloroplast and Eyespot

Our *G. stigmatica* culture has been kept for more than two years without prey, which validates its permanent possession of chloroplast. This differs from the temporary chloroplast reported in kleptoplastic sp. derived from free-living haptophytes (Gast et al. 2007; Nézan et al. 2014).

Three enveloping membranes of the peridinin-type chloroplast have been commonly reported in dinoflagellates (e.g., Dodge 1968). However, two enveloping membranes were found in few dinoflagellates, e.g., *Polykrikos lebourae* Herdman, *Gambierdiscus toxicus* Adachi and Fukuyo and *Prorocentrum* spp. (Dodge and Bibby 1973; Durand and Berkaloff 1985; Hoppenrath and Leander 2007; Kowallik 1969; details in Schnepf and Elbrächter 1999). For the 19′-AF-type chloroplast in the Kareniaceae, on the other hand, the double-membrane was reported in *Asterodinium gracile*, *Karlodinium zhouanum* Z. Luo et H. Gu and *Takayama xiamenensis* H. Gu (Benico et al. 2019; Gu et al. 2013; Luo et al. 2018). Although the chloroplast-type is different in *G. stigmatica*, the structure of chloroplast envelope shows a similarity to the 19′-AF-type chloroplast in the Kareniaceae.

The presence of an eyespot in *G. stigmatica* is the first report in the Kareniaceae. The eyespot type A is not common in marine unarmored dinoflagellates, e.g., *Amphidinium cupulatisquama* Tamura, Takano et Horiguchi, *Cochlodinium fulvescens* Iwataki, Kawami et Matsuoka, and *Cochlodinium polykrikoides* Margalef (Iwataki et al. 2007, 2010, 2015; Tamura et al. 2009), although it is more common in freshwater peridinioid dinoflagellates (e.g., Calado et al. 1999; Craveiro et al. 2009, 2011, 2015; Hansen and Flaim 2007). In *A. cupulatisquama* and *C. polykrikoides*, the osmiophilic globules of the eyespot type A form a single and double rows, respectively, and both are located in the dorsal side (Iwataki et al. 2010; Tamura et al. 2009). Other eyespot types, i.e., type B in *Dactylodinium pterobelotum* Kazuya Takahashi, Moestrup et Iwataki, type D in the Kryptoperidiniaceae with diatom symbiont (= dinotoms), and type E in the Suessiaceae, have been commonly reported from marine waters, and their ultrastructures are clearly different from the type A in *G. stigmatica* (e.g., Hansen and Daugbjerg 2009; Lum et al. 2019; Moestrup and Daugbjerg 2007; Moestrup et al. 2009a, 2009b; Takahashi et al. 2014, 2017).

Chloroplast Acquisition and Loss in the Kareniaceae

The occurrence of a peridinin-type chloroplast in *G. stigmatica* is unique within the Kareniaceae, and its origin in this particular dinoflagellate is therefore of considerable interest. Phylogenies of chloroplast- and nucleus-encoded genes, however, were not able to demonstrate the definitive evolutionary history of chloroplast acquisition/loss in the Kareniaceae. Four possible hypotheses A–D (Fig. 9) are provided below, and their probabilities are discussed with the currently available information.

Hypothesis A (Fig. 9A): *G. stigmatica* branched first in the Kareniaceae, and retained the peridinin-type chloroplast derived from the common ancestor in the family. After the loss of chloroplast, kleptoplastic sp. obtained the kleptochloroplast, and *Karenia*, *Karlodinium* and *Takayama* acquired the 19′-AF-type chloroplast once from a haptophyte. This scenario is plausible in terms of the fewest chloroplast replacement events; however, the host ITS and LSU rDNA phylogenies of *G. stigmatica* and kleptoplastic sp. do not support this branching order (Gast et al. 2006; Nézan et al. 2014).

Hypothesis B (Fig. 9B): *G. stigmatica* retained the peridinin-type chloroplast from the common ancestor, while the 19′-AF-type chloroplasts were acquired at least twice independently, in *Karenia* and in *Karlodinium/Takayama*. This agrees with the host phylogeny, but chloroplast phylogenies suggested a single origin, or at least similar origins, of the 19′-AF-type chloroplasts in the family (e.g.,

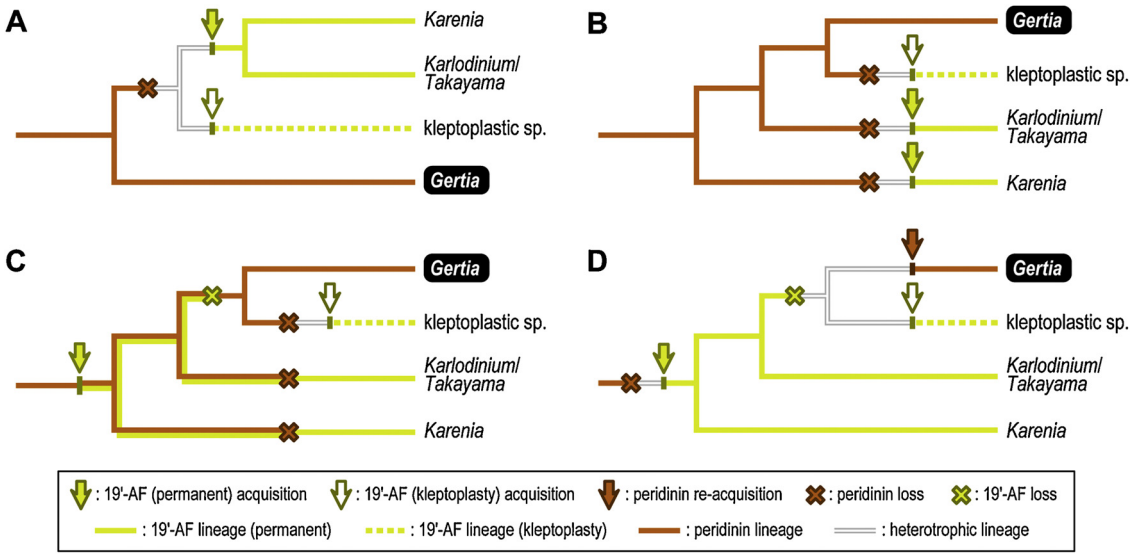

Figure 9. Four hypotheses A–D of chloroplast replacing process in the Kareniaceae assumed by phylogenies based on nucleus- and chloroplast-encoded DNAs. Tree topologies among A–D are different only in the deepest root position. **A.** Root by *Gertia*, **B–D.** Root by *Karenia*. The topology of B–D was based on ITS and LSU phylogenies.

Gabrielsen et al. 2011; Takishita et al. 2004, 2005; Tengs et al. 2000).

Hypothesis C (Fig. 9C): *G. stigmatica* retained the peridinin-type chloroplast from the common ancestor, which was also kept in other kareniaceans after the acquisition of 19′-AF-type chloroplast. This scenario agrees with the host and chloroplast phylogenies. However, this is unlikely because there exists no report of other dinoflagellates maintaining two permanent chloroplasts of different origins. Moreover, in the dinoflagellates with kleptochloroplast, e.g., *Amylax*, *Dinophysis*, *Nusuttodinium* and kleptoplastic sp., the co-existing permanent chloroplasts have never been reported (Gast et al. 2007; Koike and Takishita 2008; Takano et al. 2014; Zapata et al. 2012). The vestigial chloroplast of peridinin-type, the eyespot type D, coexists with an endosymbiotic diatom in kryptoperidiniaceans (= dinotoms) (Dodge 1984; Hehenberger et al. 2014; Moestrup and Daugbjerg 2007; Schnepf and Elbrächter 1999), but is no longer a photosynthetic organelle. The vestigial chloroplast of 19′-AF-type was not found in *G. stigmatica*, and vice versa in *Karenia/Karlodinium/Takayama* under TEM.

Hypothesis D (Fig. 9D): *G. stigmatica* newly acquired the peridinin-type chloroplast from another dinoflagellate, after an acquisition and loss of the 19′-AF-type common in the Kareniaceae. This scenario is compatible with both the host and chloroplast phylogenies, and plausible in terms of fewer chloroplast replacements. However, the particular dinoflagellate of the chloroplast origin was not resolved by our chloroplast phylogeny, and the re-acquisition of the peridinin-type chloroplast has not been reported in any other dinoflagellates. This hypothesis requires further supporting information (e.g., photosynthesis-related genes of the 19′-AF-type) yet to be explored in *G. stigmatica*.

Gertia stigmatica with the straight ASC is obviously related to the Kareniaceae; however, the chloroplast containing peridinin is the first report in the family, and the ultrastructure (double enveloping membrane) and phylogenetic traits (long branch in *psbA*, *psbC* and *psbD*) are also unusual among the peridinin-type chloroplasts. These unique ultrastructural and molecular modifications suggest an unusual event in the chloroplast evolution.

Methods

Culture: A strain of *Gertia stigmatica* gen. et sp. nov. (mdd472-kt strain) originated from a surface seawater off the coast of Manazuru, Sagami Bay, Japan (35°09′N, 139°10′E) in October 2016. *Heterocapsa circularisquama* and *Karenia mikimotoi* cultures used in pigment analyses were collected from Mikawa Bay, Japan in 2018, and from Manila Bay, Philippines in 2018, respectively. 500 mL of surface water obtained was prescreened by using a 20 μm mesh, and gently concentrated by gravity filtration using a 5 μm membrane filter. An unialgal strain was established by capillary pipetting into half strength of IMK medium (Wako, Tokyo, Japan) with salinity adjusted to

30, and it was maintained in the same medium at 20 °C in a 12:12 h light:dark regime under 40–50 μmol photons m^{-2} s^{-1}. The strain was deposited at the Microbial Culture Collection at National Institute for Environmental Studies (NIES) in Japan with a culture number NIES-4330.

Light microscopy: Cells were examined using a Zeiss Axioskop 2 (Carl Zeiss, Göttingen, Germany) light microscope fitted with an epifluorescence device. Micrographs were taken with a digital camera Zeiss Axiocam HRc (Carl Zeiss, Göttingen, Germany). Cell measurements were conducted using the micrographs. Autofluorescence of chloroplast was observed with Blue excitation of the device. To observe the fluorescence of nuclei, cells were fixed with 2.5% glutaraldehyde (final concentration), stained with 1:10,000 SYBR Green (Invitrogen, Thermo Fisher Scientific, Massachusetts, USA) and observed under Blue excitation.

Scanning electron microscopy: Cells were fixed in 1.0–1.2% OsO_4 (w/v) solution on a poly-L-lysine-coated SEM plate for 10 min at room temperature. After rinsing twice in distilled water for 30 min each, cells were dehydrated through an ethanol series of 30%, 50%, 75%, 90% and 95% for 10 min each, and twice of pure ethanol for 30 min each. The ethanol was replaced with isoamyl acetate and dried using a critical point dryer JEOL JCPD-5 (JEOL, Tokyo, Japan). The plate with attaching cells was mounted onto an SEM stub, sputter-coated with platinum and observed with an S-4800 (HITACHI, Tokyo, Japan) at an acceleration voltage of 1.0 kV.

Transmission electron microscopy: For pre-fixation of cells, three different schedules were used (schedule 1–3). Schedule 1 was performed in a mixture of 2% (v/v) glutaraldehyde and 2% (v/v) of paraformaldehyde made up in a 0.2 M Na-cacodylate buffer with 0.2 M sucrose (final concentrations) for 40 min on ice. Schedule 2 was in a 2% (v/v) glutaraldehyde made up in 0.2 M Na-cacodylate buffer with 0.2 M sucrose (final concentrations) for 30 min on ice. Schedule 3 was in a mixture of 2% (v/v) glutaraldehyde and 0.1% (v/v) OsO_4 made up in 0.1 M Na-cacodylate buffer (final concentrations) for 30 min on ice. After pre-fixation cells were centrifuged into a pellet, and for schedule 1 and schedule 2 they were rinsed with three changes of decreasing sucrose concentration; 0.2 M, 0.1 M and pure buffer, while for schedule 3 they were rinsed with three changes of pure buffer for 10 min each, and for all three schedules final rinse with twice of pure buffer for 30–60 min each was done. Post-fixation was performed by a 1.5% (w/v) OsO_4 in 0.05 M Na-cacodylate buffer for schedule 1, 1.25% (w/v) OsO_4 in 0.075 M Na-cacodylate buffer for schedule 2 and 3, for overnight at room temperature. The fixed cells were dehydrated in an ethanol series of 30%, 50%, 75%, 90% and 95% for 10–15 min each, and twice of pure ethanol for 30 min each. Replacement of ethanol was carried out using 1:1 mixture of ethanol and propylene oxide, and subsequent twice of pure propylene oxide. Cells were left overnight in a 1:1 mixture of propylene oxide and low viscosity resin (EM Japan, Tokyo, Japan), and subsequently put into twice of pure resin for 8 h each. Resin was polymerized at 70 °C for 12 h. The TEM blocks were sectioned by using an Ultracut S UTC ultramicrotome (Leica Microsystems, Wetzlar, Germany) with a diamond knife. Sections were mounted on Formvar-coated grids, and stained with uranyl acetate and lead citrate. Sectioned cells were examined under a JEM-1010 TEM (JEOL, Tokyo, Japan) at an acceleration voltage of 100 kV.

Schedule 1 provided a lower electron density of chloroplast matrix, showing clearer chloroplast membrane structures (i.e., bounding membranes, thylakoids) than other schedules. Most amphiesmal vesicles, and even some cell membranes were lost. Schedule 2 generally preserved many internal structures except amphiesmal vesicles. Schedule 3 preserved amphiesmal vesicles, but chloroplast membranes were covered by black precipitation.

Pigment analysis: Culture strains of *G. stigmatica*, *H. circularisquama* and *Karenia mikimotoi* were filtered, and their photosynthetic pigments were extracted according to Benico et al. (2019). They were analyzed in the same setting of high performance liquid chromatography (HPLC) system used in Benico et al. (2019). Peaks of pigments were identified by referring the retention times and absorption spectra of standards (Danish Hydraulic Institute, Hørsholm, Denmark) and their literature data (Roy et al. 2011).

Phylogenetic analysis: To amplify nucleus-encoded ITS and LSU rDNA, cells of *G. stigmatica* and *H. circularisquama* disrupted using distilled water were used directly for polymerase chain reaction (PCR) template (Takahashi et al. 2015). To amplify nucleus-encoded SSU rDNA of this species, hexadecyltrimethylammonium bromide (CTAB) method was used for preparation of PCR template (Takahashi et al. 2015). Ex Taq polymerase (Takara, Shiga, Japan) was used for PCR. Details of the cycling conditions and primer sets for PCR are described in Takahashi et al. (2015). To amplify chloroplast-encoded genes, total DNAs of *G. stigmatica* were extracted using CTAB method, and used for PCR. Primers for *psbA*, *psbC*, *psbD*, 16S rDNA and *rbcL* designated with a reference of peridinin-type dinoflagellates and kareniaceans are shown in Table S1, and only amplification of *psbA*, *psbC* and *psbD* was successful. Primer sets used for PCR were bAf2d and bAr6d for *psbA*, bCf1k and bCr2d for *psbC*, bDf1d and bDr6d for *psbD* (Table S1). DNA polymerase used for amplification was Ex Taq (Takara, Shiga, Japan) for *psbC*/*psbD* and MightyAmp (Takara, Shiga, Japan) for *psbA*. Final volume of 10 μL PCR mix was reacted with the thermal condition as follows; for *psbA*, an initial denaturation step at 98 °C for 2 min, followed by 35 cycles of 3 steps, 98 °C for 10 s, 55 °C for 15 s and 68 °C for 2.5 min, and finally an elongation step of 68 °C for 6 min; for *psbC* and *psbD*, an initial denaturation step at 94 °C for 1 min, followed by 42–47 cycles of 3 steps, 94 °C for 20 s, 47 °C for 30 s and 72 °C for 2–2.5 min, and finally an elongation step of 72 °C for 7 min. PCR products of rDNA, *psbA*, *psbC* and *psbD* were purified using QIAquick PCR Purification Kit (Qiagen Genomics, Both-ell, WA, USA) following the manufacturer's protocol. Sequencing of the amplicons using the appropriate internal primers (shown in Takahashi et al. 2015 for nucleus-encoded rDNA, in Supplementary Material Table S1 for chloroplast-encoded genes) was outsourced, following manufacture's protocol (Eurofins Genomics, Tokyo, Japan). Determined sequences were deposited in GenBank under the accession numbers LC490696 (SSU, ITS and LSU of *G. stigmatica*), LC490697 (ITS and LSU of *H. circularisquama*), LC492438 (*psbA* of *G. stigmatica*), LC492439 (*psbC* of *G. stigmatica*) and LC492440 (*psbD* of *G. stigmatica*).

To infer a host dinoflagellate phylogeny, phylogenetic trees of nucleus-encoded concatenated sequences of SSU rDNA (18S), ITS (5.8 S) and LSU (28S) rDNA (excluding a part of D2 region, Fig. 7A), SSU only (Fig. 7B; Supplementary Material Fig. S1), ITS region only (ITS1, 5.8S and ITS2 regions, Fig. 7C, Supplementary Material Fig. S2) and LSU only (including D2 region, Fig. 7D, Supplementary Material Fig. S3) were constructed. To infer chloroplast phylogeny, phylogenetic trees of *psbA*-*psbC*-*psbD* concatenated chloroplast genes (Fig. 8), *psbA* only (Supplementary Material Fig. S4), *psbC* only (Supplementary Material Fig. S5) and *psbD* only (Supplementary Material Fig. S6) were constructed. SSU, ITS and LSU sequences were obtained from GenBank, and the obviously related sequences (i.e., identical sequences after eliminating diverse regions at both terminals) were compiled

into a single sequence. For *psbA*, *psbC* and *psbD* analyses, dataset collected in Dorrell et al. (2016) was used (available in https://www.repository.cam.ac.uk/handle/1810/252774; last accessed February 17, 2019), in addition to the sequences obtained from GenBank. Accession numbers are shown after species name in the phylogenetic trees, and common tags 'CAMNT 00' before at the 8-digit numbers were omitted for transcript data sourced from iMicrobe (Figs 7, 8; Supplementary Material Figs S1–S6). Multiple alignment including the determined sequences was constructed using Clustal X (ver.1.8) computer algorithm, and obviously misaligned locations were checked by eyes and manually corrected. Phylogenetic trees were constructed by Bayesian inference (BI) using a MrBayes v. 3.1.2 software (Ronquist and Huelsenbeck 2003), and maximum likelihood (ML) analyses using a Molecular Evolutionary Genetics Analysis version 6.0 (MEGA 6) (Tamura et al. 2013). Best substitution models were selected by a MrModeltest v. 2.3 software (Nylander 2008) for BI, and by the MEGA6 for ML. Using appropriate number (500,000–10,000,000) of the Markov Chain Monte Carlo (MCMC) generations with four chains, posterior probabilities (PP) of BI tree topology were calculated, to confirm the convergence of calculation when the average standard deviations of split frequencies were below 0.01. The validity of branching order in ML trees was estimated by bootstrap support (BS) values with 500 replicates. Detailed analytical settings including the number of operational taxonomic units (OTUs), the number of compared characters, base pair substitution models, and the number of MCMC generations are described in figure legends (Figs 7, 8; Supplementary Material Figs S1–S6).

Acknowledgements

We appreciate Dr. Shinji Shimode of Yokohama National University and Ms. Shiori Otake of University of Tokyo for their sampling assistance. Dr. Kazutaka Takahashi of University of Tokyo provided experimental tools including maintenance of culture strain, molecular analysis and EM preparation. Dr. Fumiko Ishizuna of University of Tokyo provided assistance on TEM. Dr. Tomoyo Katayama and Mr. Shota Takino of University of Tokyo and Dr. Takashi Yoshikawa of Tokai University provided assistance on HPLC. Dr. Yuji Inagaki and Dr. Eriko Matsuo of Tsukuba University provided assistance on phylogenetic analyses. This work was partially supported by Grants-in-Aid for Scientific Research, Japan Society for the Promotion of Science(JSPS) KAKENHI Grant Numbers 25304029 and 15H04533, and JSPS Core-to-Core Program, B. Asia-Africa Science Platforms.

Appendix A. Supplementary Data

Supplementary material related to this article can be found, in the online version, at doi:https://doi.org/10.1016/j.protis.2019.125680.

References

Al-Kandari MA, Highfield AC, Hall MJ, Hayes P, Schroeder DC (2011) Molecular tools separate harmful algal bloom species, *Karenia mikimotoi*, from different geographical regions into distinct sub-groups. Harmful Algae **10**:636–643

Benico GA, Takahashi K, Lum WM, Iwataki M (2019) Morphological variation, ultrastructure, pigment composition and phylogeny of a star-shaped dinoflagellate *Asterodinium gracile* (Kareniaceae, Dinophyceae). Phycologia **58**:405–418

Bergholtz T, Daugbjerg N, Moestrup Ø, Fernández-Tejedor M (2005) On the identity of *Karlodinium veneficum* and description of *Karlodinium armiger* sp. nov. (Dinophyceae), based on light and electron microscopy, nuclear-encoded LSU rDNA, and pigment composition. J Phycol **42**:170–193

Bjørnland T, Tangen K (1979) Pigmentation and morphology of a marine *Gyrodinium* (Dinophyceae) with a major carotenoid different from peridinin and fucoxanthin. J Phycol **15**:457–463

Calado AJ, Hansen G, Moestrup Ø (1999) Architecture of the flagellar apparatus and related structures in the type species of *Peridinium*, *P. cinctum* (Dinophyceae). Eur J Phycol **34**:179–191

Chang FH, Gall M (2013) Pigment compositions and toxic effects of three harmful *Karenia* species, *Karenia concordia*, *Karenia brevisulcata* and *Karenia mikimotoi* (Gymnodiniales, Dinophyceae), on rotifers and brine shrimps. Harmful Algae **27**:113–120

Craveiro SC, Calado AJ, Daugbjerg N, Moestrup Ø (2009) Ultrastructure and LSU rDNA-based revision of *Peridinium* group palatinum (Dinophyceae) with the description of *Palatinus* gen. nov. J Phycol **45**:1175–1194

Craveiro SC, Daugbjerg N, Moestrup Ø, Calado AJ (2015) Fine-structural characterization and phylogeny of *Peridinium polonicum*, type species of the recently described genus *Naiadinium* (Dinophyceae). Europ J Protistol **51**:259–279

Craveiro SC, Calado AJ, Daugbjerg N, Hansen G, Moestrup Ø (2011) Ultrastructure and LSU rDNA-based phylogeny of *Peridinium lomnickii* and description of *Chimonodinium* gen. nov. (Dinophyceae). Protist **162**:590–615

Dai X, Lu D, Guan W, Wang H, He P, Xia P, Yang H (2014) Newly recorded *Karlodinium veneficum* dinoflagellate blooms in stratified water of the East China Sea. Deep-Sea Res II **101**:237–243

Daugbjerg N, Hansen G, Larsen J, Moestrup Ø (2000) Phylogeny of some of the major genera of dinoflagellates based on ultrastructure and partial LSU rDNA sequence data, including the erection of three new genera of unarmoured dinoflagellates. Phycologia **39**:302–317

de Salas MF, Bolch CJ, Hallegraeff GM (2004) *Karenia umbella* sp. nov. (Gymnodiniales, Dinophyceae), a new potentially ichthyotoxic dinoflagellate species from Tasmania, Australia. Phycologia **43**:166–175

de Salas MF, Bolch CJ, Hallegraeff GM (2005) *Karlodinium australe* sp. nov. (Gymnodiniales, Dinophyceae), a new potentially ichthyotoxic unarmoured dinoflagellate from lagoonal habitats of south-eastern Australia. Phycologia **44**:640–650

de Salas MF, Laza-Martínez A, Hallegraeff GM (2008) Novel unarmored dinoflagellates from the toxigenic family Kareni-

aceae (Gymnodiniales): five new species of *Karlodinium* and one new *Takayama* from the Australian sector of the Southern Ocean. J Phycol **44**:241–257

de Salas MF, Bolch CJ, Botes L, Nash G, Wright SW, Hallegraeff GM (2003) *Takayama* gen. nov. (Gymnodiniales, Dinophyceae), a new genus of unarmored dinoflagellates with sigmoid apical grooves, including the description of two new species. J Phycol **39**:1233–1246

Dodge JD (1968) The fine structure of chloroplasts and pyrenoids in some marine dinoflagellates. J Cell Sci **3**:41–48

Dodge JD (1984) The functional and phylogenetic significance of dinoflagellate eyespots. Biosystems **16**:259–267

Dodge JD, Bibby BT (1973) The Prorocentrales (Dinophyceae): I. A comparative account of fine structure in the genera *Prorocentrum* and *Exuviaella*. Bot J Linn Soc **67**:175–187

Dorrell RG, Klinger CM, Newby RJ, Butterfield ER, Richardson E, Dacks JB, Howe CJ, Nisbet ER, Bowler C (2016) Progressive and biased divergent evolution underpins the origin and diversification of peridinin dinoflagellate plastids. Mol Biol Evol **34**:361–379

Durand M, Berkaloff C (1985) Pigment composition and chloroplast organization of *Gambierdiscus toxicus* Adachi and Fukuyo (Dinophyceae). Phycologia **24**:217–223

Elbrächter M, Schnepf E (1996) *Gymnodinium chlorophorum*, a new, green, bloom-forming dinoflagellate (Gymnodiniales, Dinophyceae) with a vestigial prasinophyte endosymbiont. Phycologia **35**:381–393

Gabrielsen TM, Minge MA, Espelund M, Tooming-Klunderud A, Patil V, Nederbragt AJ, Otis C, Turmel M, Shalchian-Tabrizi K, Lemieux C, Jakobsen KS (2011) Genome evolution of a tertiary dinoflagellate plastid. PLoS ONE **6**, e19132

Gast RJ, Moran DM, Dennett MR, Caron DA (2007) Kleptoplasty in an Antarctic dinoflagellate: caught in evolutionary transition? Environ Microbiol **9**:39–45

Gast RJ, Moran DM, Beaudoin DJ, Blythe JN, Dennett MR, Caron DA (2006) Abundance of a novel dinoflagellate phylotype in the Ross Sea, Antarctica. J Phycol **42**:233–242

Gómez F (2006) The dinoflagellate genera *Brachidinium*, *Asterodinium*, *Microceratium* and *Karenia* in the open SE Pacific Ocean. Algae **21**:445–452

Gómez F, Nagahama J, Takayama H, Furuya K (2005) Is *Karenia* a synonym of *Asterodinium-Brachidinium* (Gymnodiniales, Dinophyceae)? Acta Bot Croatica **64**:263–274

Gómez F, Qiu D, Dodge JD, Lopes RM, Lin S (2016) Morphological and molecular characterization of *Ptychodiscus noctiluca* revealed the polyphyletic nature of the order Ptychodiscales (Dinophyceae). J Phycol **52**:793–805

Gu H, Luo Z, Zhang X, Xu B, Fang Q (2013) Morphology, ultrastructure and phylogeny of *Takayama xiamenensis* sp. nov. (Gymnodiniales, Dinophyceae) from the East China Sea. Phycologia **52**:256–265

Hansen G, Daugbjerg N (2009) *Symbiodinium natans* sp. nov.: A "free-living" dinoflagellate from Tenerife (Northeast-Atlantic Ocean). J Phycol **45**:251–263

Hansen G, Flaim G (2007) Dinoflagellates of the Trentino province, Italy. J Limnol **66**:107–141

Hansen G, Moestrup Ø (2005) Flagellar apparatus and nuclear chambers of the green dinoflagellate *Gymnodinium chlorophorum*. Phycol Res **53**:169–181

Hansen G, Botes L, de Salas M (2007) Ultrastructure and large subunit rDNA sequences of *Lepidodinium viride* reveal a close relationship to *Lepidodinium chlorophorum* comb. nov. (= *Gymnodinium chlorophorum*). Phycol Res **55**:25–41

Hansen G, Daugbjerg N, Henriksen P (2000) Comparative study of *Gymnodinium mikimotoi* and *Gymnodinium aureolum*, comb. nov. (= *Gyrodinium aureolum*) based on morphology, pigment composition, and molecular data. J Phycol **36**:394–410

Haywood AJ, Steidinger KA, Truby EW, Bergquist PR, Bergquist PL, Adamson J, Mackenzie L (2004) Comparative morphology and molecular phylogenetic analysis of three new species of the genus *Karenia* (Dinophyceae) from New Zealand. J Phycol **40**:165–179

Hehenberger E, Imanian B, Burki F, Keeling PJ (2014) Evidence for the retention of two evolutionary distinct plastids in dinoflagellates with diatom endosymbionts. Genome Biol Evol **6**:2321–2334

Henrichs DW, Sosik HM, Olson RJ, Campbell L (2011) Phylogenetic analysis of *Brachidinium capitatum* (Dinophyceae) from the Gulf of Mexico indicates membership in the Kareniaceae. J Phycol **47**:366–374

Hoppenrath M, Leander BS (2007) Morphology and phylogeny of the pseudocolonial dinoflagellates *Polykrikos lebourae* and *Polykrikos herdmanae* n. sp. Protist **158**:209–227

Ishida K, Green BR (2002) Second- and third-hand chloroplasts in dinoflagellates: phylogeny of oxygen-evolving enhancer 1 (PsbO) protein reveals replacement of a nuclear-encoded plastid gene by that of a haptophyte tertiary endosymbiont. Proc Natl Acad Sci USA **99**:9294–9299

Iwataki M, Kawami H, Matsuoka K (2007) *Cochlodinium fulvescens* sp. nov. (Gymnodiniales, Dinophyceae), a new chain-forming unarmored dinoflagellate from Asian coasts. Phycol Res **55**:231–239

Iwataki M, Hansen G, Moestrup Ø, Matsuoka K (2010) Ultrastructure of the harmful unarmored dinoflagellate *Cochlodinium polykrikoides* (Dinophyceae) with reference to the apical groove and flagellar apparatus. J Eukaryot Microbiol **57**:308–321

Iwataki M, Takayama H, Takahashi K, Matsuoka K (2015) Taxonomy and Distribution of the Unarmored Dinoflagellates *Cochlodinium polykrikoides* and *C. fulvescens*. In Ohtsuka S, Suzaki T, Horiguchi T, Not F (eds) Marine Protists: Diversity and Dynamics. Springer, Tokyo, pp 551–565

Kofoid CA, Swezy O (1921) The Free-Living Unarmoured Dinoflagellata. Mem Univ Calif **5**:1–564

Koike K, Takishita K (2008) Anucleated cryptophyte vestiges in the gonyaulacalean dinoflagellates *Amylax buxus* and *Amylax triacantha* (Dinophyceae). Phycol Res **56**:301–311

Kowallik K (1969) The crystal lattice of the pyrenoid matrix of *Prorocentrum micans*. J Cell Sci **5**:251–269

Larsen J (1994) Unarmoured dinoflagellates from Australian waters I. The genus *Gymnodinium* (Gymnodiniales, Dinophyceae). Phycologia **33**:24–33

Leong SCY, Lim LP, Chew SM, Kok JWK, Teo SLM (2015) Three new records of dinoflagellates in Singapore's coastal waters, with observations on environmental conditions associated with microalgal growth in the Johor Straits. Raffles Bull Zool Suppl **31**:24–36

Lim HC, Leaw CP, Tan TH, Kon NF, Yek LH, Hii KS, Teng ST, Razali RM, Usup G, Iwataki M, Lim PT (2014) A bloom of *Karlodinium australe* (Gymnodiniales, Dinophyceae) associated with mass mortality of cage-cultured fishes in West Johor Strait, Malaysia. Harmful Algae **40**:51–62

Lum WM, Takahashi K, Benico B, Takayama H, Iwataki M (2019) *Dactylodinium arachnoides* sp. nov. (Borghiellaceae, Dinophyceae): a new marine dinoflagellate with a loop-shaped apical structure complex and tubular membranous extrusomes. Phycologia, http://dx.doi.org/10.1080/00318884.2019.1658399

Luo Z, Wang L, Chan L, Lu S, Gu H (2018) *Karlodinium zhouanum*, a new dinoflagellate species from China, and molecular phylogeny of *Karenia digitata* and *Karenia longicanalis* (Gymnodiniales, Dinophyceae). Phycologia **57**:401–412

Moestrup Ø, Daugbjerg N (2007) On Dinoflagellate Phylogeny and Classification. In Brodie J, Lewis J (eds) Unravelling the Algae: The Past, Present, and Future of Algae Systematics. Systematics Association Special Volumes **Vol. 75**. CRC Press, London, pp 215–230

Moestrup Ø, Lindberg K, Daugbjerg N (2009a) Studies on woloszynskioid dinoflagellates IV: The genus *Biecheleria* gen. nov. Phycol Res **57**:203–220

Moestrup Ø, Lindberg K, Daugbjerg N (2009b) Studies on woloszynskioid dinoflagellates V. Ultrastructure of *Biecheleriopsis* gen. nov. Phycol Res **57**:221–237

Nézan E, Siano R, Boulben S, Six C, Bilien G, Chèze K, Duval A, Panse SL, Quéré J, Chomérat N (2014) Genetic diversity of the harmful family Kareniaceae (Gymnodiniales, Dinophyceae) in France, with the description of *Karlodinium gentienii* sp. nov.: A new potentially toxic dinoflagellate. Harmful Algae **40**:75–91

Nylander JAA (2008) MrModeltest v2. 3. Evolutionary Biology Centre, Uppsala University, Norbyvägen, Uppsala, Sweden

Onoue Y, Nozawa K, Kumanda K, Takeda K, Aramaki T (1985) Occurrence of a toxic dinoflagellate "*Gymnodinium*-type '84 K'" in Kagoshima Bay. Bull Jpn Soc Sci Fish **51**:1567

Ronquist F, Huelsenbeck JP (2003) MRBAYES 3: Bayesian phylogenetic inference under mixed models. Bioinformatics **19**:1572–1574

Roy S, Llewellyn CA, Egeland ES, Johnsen G (eds) Phytoplankton Pigments, Characterization, Chemotaxonomy and Applications in Oceanography. Cambridge Environmental Chemistry, Cambridge University, Cambridge, UK, 845 pp

Schiller J (1933) Dinoflagellatae (Peridineae). In Rabenhorst L (ed) Kryptogamen-Flora von Deutschland, Österreich und der Schweiz, 2. Aufl. X. Band 3. Abt. 1 Teil. Akademische Verlagsgesellschaft, MGH, Leipzig, pp 1–617

Schnepf E, Elbrächter M (1999) Dinophyte chloroplasts and phylogeny-A review. Grana **38**:81–97

Takahashi K, Sarai C, Iwataki M (2014) Morphology of two marine woloszynskioid dinoflagellates, *Biecheleria brevisulcata* sp. nov. and *Biecheleriopsis adriatica* (Suessiaceae, Dinophyceae), from Japanese coasts. Phycologia **53**:52–65

Takahashi K, Moestrup Ø, Jordan RW, Iwataki M (2015) Two new freshwater woloszynskioids *Asulcocephalium miricentonis* gen. et sp. nov. and *Leiocephalium pseudosanguineum* gen. et sp. nov. (Suessiaceae, Dinophyceae) lacking an apical furrow apparatus. Protist **166**:638–658

Takahashi K, Moestrup Ø, Wada M, Ishimatsu A, Nguyen NV, Fukuyo Y, Iwataki M (2017) *Dactylodinium pterobelotum* gen. et sp. nov, a new marine woloszynskioid dinoflagellate positioned between the two families Borghiellaceae and Suessiaceae. J Phycol **53**:1223–1240

Takano Y, Yamaguchi H, Inouye I, Moestrup Ø, Horiguchi T (2014) Phylogeny of five species of *Nusuttodinium* gen. nov. (Dinophyceae), a genus of unarmoured kleptoplastidic dinoflagellates. Protist **165**:759–778

Takayama H (1981) Observations on two species of *Gymnodinium* with scanning electron microscopy. Bull Plankton Soc Jpn **28**:121–129

Takayama H (1985) Apical grooves of unarmored dinoflagellates. Bull Plankton Soc Jpn **32**:129–140

Takayama H, Matsuoka K (1991) A reassessment of the specific characters of *Gymnodinium mikimotoi* Miyake et Kominami ex Oda and *Gymnodinium nagasakiense* Takayama et Adachi. Bull Plankton Soc Jpn **38**:53–68

Takayama H, Matsuoka K, Fukuyo Y (1998) A taxonomic study on *Gyrodinium aureolum* Hulburt (Dinophyceae) from the morphological viewpoint based on materials collected in Japanese coastal waters. Bull Plankton Soc Jpn **45**:9–19

Takishita K, Ishida K, Maruyama T (2004) Phylogeny of nuclear-encoded plastid-targeted GAPDH gene supports separate origins for the peridinin-and the fucoxanthin derivative-containing plastids of dinoflagellates. Protist **155**:447–458

Takishita K, Nakano K, Uchida A (1999) Preliminary phylogenetic analysis of plastid-encoded genes from an anomalously pigmented dinoflagellate *Gymnodinium mikimotoi* (Gymnodiniales, Dinophyta). Phycol Res **47**:257–262

Takishita K, Nakano K, Uchida A (2000) Origin of the plastid in the anomalously pigmented dinoflagellate *Gymnodinium mikimotoi* (Gymnodiniales, Dinophyta) as inferred from phylogenetic analysis based on the gene encoding the large subunit of form I-type RuBisCO. Phycol Res **48**:85–89

Takishita K, Ishida K, Ishikura M, Maruyama T (2005) Phylogeny of the *psbC* gene, coding a photo- system II component CP43, suggests separate origins for the peridinin- and the fucoxanthin derivative-containing plastids of dinoflagellates. Phycologia **44**:26–34

Tamura M, Takano Y, Horiguchi T (2009) Discovery of a novel type of body scale in the marine dinoflagellate, *Amphidinium cupulatisquama* sp. nov. (Dinophyceae). Phycol Res **57**:304–312

Tamura K, Stecher G, Peterson D, Filipski A, Kumar S (2013) MEGA6: Molecular Evolutionary Genetics Analysis version 6. 0. Mol Biol Evol **30**:2725–3729

Tangen K, Bjørnland T (1981) Observations on pigments and morphology of *Gyrodinium aureolum* Hulburt, a marine dinoflagellate containing 19'-hexanoyloxyfucoxanthin as the main carotenoid. J Plankton Res **3**:389–401

Tengs T, Dahlberg OJ, Shalchian-Tabrizi K, Klaveness D, Rudi K, Delwiche CF, Jakobsen KS (2000) Phylogenetic analyses indicate that the 19'-hexanoyloxy-fucoxanthin-containing dinoflagellates have tertiary plastids of haptophyte origin. Mol Biol Evol **17**:718–729

Waller RF, Koreny L (2017) Plastid Complexity in Dinoflagellates: A Picture of Gains, Losses, Replacements and Revisions. In Hirakawa Y (ed) Advances in Botanical Research **Vol. 84**. Academic Press, Cambridge, pp 105–143

Watanabe MM, Suda S, Inouye I, Sawaguchi T, Chihara M (1990) *Lepidodinium viride* gen. et sp. nov. (Gymnodiniales, Dinophyta), a green dinoflagellate with a chlorophyll *a*- and *b*-containing endosymbiont. J Phycol **26**:741–751

Watanabe MM, Takeda Y, Sasa Y, Inouye I, Suda S, Sawaguchi T, Chihara M (1987) A green dinoflagellate with chlorophylls *a* and *b*: morphology, fine structure of the chloroplast and chlorophyll composition. J Phycol **23**: 382–389

Yang ZB, Hodgkiss IJ, Hansen G (2001) *Karenia longicanalis*sp. nov. (Dinophyceae): a new bloom-forming species isolated from Hong Kong, May 1998. Bot Mar **44**: 67–74

Yang ZB, Takayama H, Matsuoka K, Hodgkiss IJ (2000) *Karenia digitata* sp. nov. (Gymnodiniales, Dinophyceae), a new harmful algal bloom species from the coastal waters of west Japan and Hong Kong. Phycologia **39**:463–470

Zapata M, Fraga S, Rodríguez F, Garrido JL (2012) Pigment-based chloroplast types in dinoflagellates. Mar Ecol Prog Ser **465**:33–52